1

1   **Rapid radiation of Southern Ocean shags in response to receding sea ice**

2

3   Running title: Blue-eyed shag phylogeography

4

5   Nicolas J. Rawlence[1, *], Alexander T. Salis[1, 2], Hamish G. Spencer[1], Jonathan M. Waters[1],
6   Lachie Scarsbrook[1], Richard A. Phillips[3], Luciano Calderón[4], Timothée R. Cook[5], Charles-
7   André Bost[6], Ludovic Dutoit[1], Tania M. King[1], Juan F. Masello[7], Lisa J. Nupen[8], Petra
8   Quillfeldt[7], Norman Ratcliffe[3], Peter G. Ryan[5], Charlotte E. Till[1, 9], Martyn Kennedy[1,*]

9   [1] Department of Zoology, University of Otago, Dunedin, New Zealand.

10   [2] Australian Centre for Ancient DNA, University of Adelaide, South Australia, Australia.

11   [3] British Antarctic Survey, Natural Environment Research Council, United Kingdom.

12   [4] Instituto de Biología Agrícola de Mendoza (IBAM, CONICET-UNCuyo), Argentina.

13   [5] FitzPatrick Institute of African Ornithology, Department of Biological Sciences, University
14   of Cape Town, South Africa.

15   [6] CEBC-CNRS, UMR 7372, 405 Route de Prissé la Charrière, 79360 Villiers en Bois,
16   France.

17   [7] Justus Liebig University, Giessen, Germany.

18   [8] Organisation for Tropical Studies, Skukuza, South Africa.

19   [9] School of Human Evolution and Social Change, Arizona State University, Arizona, USA.

20

21   Prepared for submission as a research article to *Journal of Biogeography*

22

23   [*] Corresponding authors: nic.rawlence@otago.ac.nz; martyn.kennedy@otago.ac.nz

24

25   **ACKNOWLEDGEMENTS**

38

39   **ABSTRACT**

40   Aim:

41   Understanding how wild populations respond to climatic shifts is a fundamental goal of
42   biological research in a fast-changing world. The Southern Ocean represents a fascinating
43   system for assessing large-scale climate-driven biological change, as it contains extremely
44   isolated island groups within a predominantly westerly, circumpolar wind and current system.
45   The blue-eyed shags (*Leucocarbo* spp.) represent a paradoxical Southern Ocean seabird
46   radiation; a circumpolar distribution implies strong dispersal capacity yet their speciose
47   nature suggests local adaptation and isolation. Here we use genetic tools in an attempt to
48   resolve this paradox.

49   Location:

50   Southern Ocean.

51   Taxa:

52   17 species and subspecies of blue-eyed shags (*Leucocarbo* spp.) across the geographical
53   distribution of the genus.

54   Methods:

55   Here we use mitochondrial and nuclear sequence data to conduct the first global genetic
56   analysis of this group using a temporal phylogenetic framework to test for rapid speciation.

57   Results:

58   Our analysis reveals remarkably shallow evolutionary histories among island-endemic
59   lineages, consistent with a recent high-latitude circumpolar radiation. This rapid sub-
60   Antarctic expansion contrasts with significantly deeper lineages detected in more temperate
61   regions such as South America and New Zealand that may have acted as glacial refugia. The
62   dynamic history of high-latitude expansions is further supported by ancestral demographic
63   and biogeographic reconstructions.

64   Main conclusions:

65   The circumpolar distribution of blue-eyed shags, and their highly dynamic evolutionary
66   history, potentially make *Leucocarbo* a strong sentinel of past and ongoing Southern Ocean
67   ecosystem change given their sensitivity to climatic impacts.

68

69   **Keywords** Biogeography, climate change, cormorant, *Leucocarbo*, speciation, Southern
70   Ocean, sub-Antarctic

71

72

1. INTRODUCTION

Understanding how wild populations respond to climatic shifts represents a key goal of biological research in a fast-changing world (Parmesan & Yohe, 2003; Chen et al., 2011). Climate change can underpin major shifts in the distribution and diversity of biological assemblages, with glacial-interglacial cycles thought to have driven dramatic changes in species distributions across many regions of the globe (Davis & Shaw, 2001). The biogeographic responses of Northern Hemisphere biota to Quaternary climate shifts, and associated ice sheet dynamics, are relatively well studied (Hewitt, 2000; Maggs et al., 2008). By contrast, climate-driven shifts involving Southern Hemisphere taxa, especially those inhabiting the Southern Ocean, remain less understood (Fraser et al., 2009; Fraser et al., 2010; Fraser et al., 2012; Cole et al., 2019).

The Southern Ocean represents a fascinating system for assessing large-scale climate-driven biological change, as it contains multiple groups of extremely isolated oceanic islands within the predominantly westerly wind and current system encircling Antarctica (Fraser et al., 2012). Understanding the evolutionary dynamics of these unique island ecosystems, and of their distinctive endemic taxa, is particularly important in the context of the region's dynamic climatic history. Specifically, geological and biological evidence together indicate that, during recent glacial maxima, several of these outlying island groups (e.g., South Georgia, Kerguelen, Heard, Crozet, Macquarie [itself only ~700,000 years old]) were encompassed by winter sea ice for thousands of years (Fig. 1) (Gersonde et al., 2005; Fraser et al., 2009; Trucchi et al., 2014) and in some cases potentially covered in ice and snow (Hodgson et al., 2014). Indeed, Heard Island was permanently covered in ice during the Last Glacial Maximum (Ehlers et al., 2011).

The Pleistocene Ice Age (2.58 – 0.01 Mya) was characterized by repeated glacial-interglacial cycles (Ehlers et al., 2011). Major deglaciation events can provide significant ecological opportunities for surviving species (Fraser et al., 2018). Indeed, recent genetic data suggest that some highly-dispersive Southern Ocean species or communities have, at different timescales, responded rapidly to colonize newly vacant habitats arising from such climate-driven ecosystem change (de Bruyn et al., 2009; Fraser et al., 2009; Fraser et al., 2010; Nikula et al., 2010; Fraser et al., 2011; Fraser et al., 2012; Fraser et al., 2018; Gonzalez-Wevar et al., 2017; Gonzalez-Wevar et al., 2018; Carrea et al., 2019; Cole et al., 2019; Gonzalez-Wevar et al., 2019; Rexer-Huber et al., 2019; Baird et al. 2021). In some cases, low levels of dispersal may permit postglacial recolonization, but may fail to provide sufficient gene flow to prevent speciation. Such scenarios are exemplified by the terrestrial Ectemnorhinini weevils and the subtidal limpet genus *Nacella,* which exhibit island-level endemism around the entire Southern Ocean, with divergences dating to the Plio-Pleistocene boundary (~2.58 Mya) and the mid-Pleistocene (0.25-0.6 Mya), respectively (Gonzalez-Wevar et al., 2017; Gonzalez-Wevar et al., 2019; Baird et al., 2021).

At the opposite end of the scale, the highly dispersive southern bull kelp (*Durvillaea antarctica*; a keystone intertidal species), and its associated rafting invertebrate communities, exhibit a 'northern richness; southern purity' model whereby disjunct high-latitude sub-Antarctic islands share anomalously low-diversity, circumpolar lineages (Fraser et al., 2009; Nikula et al., 2010; Fraser et al., 2010; Fraser et al., 2011; Fraser et al., 2012; Fraser et al., 2018; Gonzalez-Wevar et al., 2018; Cole et al., 2019). Fraser et al. (2009) hypothesized that

117   these patterns reflect recent passive post-Last Glacial Maximum (LGM) recolonization from
118   ice-free refugia facilitated by circumpolar ocean currents. The intertidal air-breathing limpets
119   *Siphonaria lateralis* and *S. fuegiensis*, which are closely associated with bull kelp, appear to
120   show a more persistent occupation of high-latitude sub-Antarctic islands, as evidenced by
121   their negligible phylogeographic structure suggesting continuing gene flow throughout their
122   range (Gonzalez-Wevar et al., 2018). Intriguingly, the highly mobile southern elephant seal
123   (*Mirounga leonina*), which exhibits a multiregional refugial pattern (de Bruyn et al., 2009)
124   (see also Rexer-Huber et al., 2019), rapidly expanded their range to newly ice-free parts of
125   the Antarctic coast (2500 km from the nearest breeding colony) 8000 years ago before
126   abandoning this new colony 1000 years ago when a grounded ice-sheet returned. These
127   apparently climate-driven patterns are mirrored to some extent by multispecies demographic
128   analyses of high-latitude penguins which reveal concordant evidence for simultaneous and
129   rapid post-LGM population expansions associated with exposure of snow-free ground on
130   which to breed (Cole et al., 2019).

131   These contrasting biogeographic responses to the Pleistocene glacial-interglacial cycles are
132   underpinned by biology. The gilled *Nacella* limpets can survive subtidally, including on the
133   Antarctic Peninsula (Gonzalez-Wevar et al., 2017; Gonzalez-Wevar et al., 2019), and are thus
134   not as affected by continual ice as more intertidal species like southern bull kelp (despite its
135   ability to passively drift onto Antarctic shores; Fraser et al., 2018), air-breathing *Siphonaria*
136   limpets (Gonzalez-Wevar et al., 2018) or southern elephant seals (de Bruyn et al. 2009).

137   Blue-eyed shags (*Leucocarbo* spp.) are an ecologically important and highly speciose group
138   of philopatric seabirds exhibiting a circumpolar Southern Ocean distribution, with 17
139   currently accepted species and subspecies (Kennedy & Spencer, 2014; Rawlence et al.,
140   2017). Many of these taxa are endemic to single island groups (Fig. 1). Additionally, the
141   small number of lineages that breed on mainland coasts typically exhibit strong
142   phylogeographic structure (Calderon et al., 2014; Kennedy & Spencer, 2014; Rawlence et al.,
143   2015; Rawlence et al., 2017). Preliminary genetic research has suggested that blue-eyed
144   shags comprise two widespread, species-rich clades: a sub-Antarctic clade encompassing
145   South America, Antarctica, and high-latitude sub-Antarctic islands; and the other occurring
146   across the New Zealand region (Fig. 1) (Kennedy & Spencer, 2014). Data from the subfossil
147   record and ancient DNA analysis suggests that at least one recently-recognized mainland
148   taxon (*L. chalconotus*) has suffered substantial loss of genetic and geographic diversity since
149   human arrival in mainland New Zealand (Rawlence et al., 2015; Rawlence et al., 2017).

150   The broad, species-rich biogeography of *Leucocarbo* presents something of a paradox.
151   Specifically, while the wide Southern Ocean distribution of the genus, incorporating
152   numerous isolated islands, implies strong dispersal capacity, the presence of numerous
153   single-island endemics suggests that such dispersal ability is insufficient to prevent
154   widespread speciation. This situation in blue-eyed shags may be somewhat akin to iconic
155   radiations described from remote archipelagic systems such as Hawaii, the Galapagos, and
156   the Canaries (Mendelson & Shaw, 2005; Shaw & Gillespie, 2016) in which the evolution of
157   island endemics has apparently been underpinned by founder speciation (Waters et al., 2013).
158   Unlike these low latitude archipelagos, however, the Southern Ocean islands have been
159   heavily impacted by recent glacial cycles (Fraser et al. 2009; Fraser et al., 2012), suggesting
160   that much of their biotic diversity may have evolved relatively recently.
161

162 Based on the distinctive Southern Ocean biogeography of *Leucocarbo* shags, we hypothesize
163 that glacial-interglacial transitions have presented crucial opportunities for rapid circumpolar
164 range expansion and founder speciation in this group. Here we present the first multigene
165 analysis of *Leucocarbo*, that includes all recognized taxa, using a temporal phylogenetic
166 framework to test for rapid radiation of this unusually speciose Southern Ocean assemblage.

167

168   2.   MATERIALS AND METHODS

169   2.1 Specimens, DNA extraction, PCR and sequencing

170 Tissue, blood, or feathers were obtained from a number of sources, covering the geographic
171 distribution of *Leucocarbo* shags (Appendix One Table S1.1-1.2). Total genomic DNA was
172 extracted using a phenol/chloroform extraction, a 5% Chelex 100 solution or the Qiagen
173 DNeasy Tissue Kit (Walsh et al., 2013; Kennedy & Spencer, 2014). Negative controls were
174 included with each extraction. For the phylogenetic dataset (using a single location per taxon,
175 except for four taxa where two locations were used and one taxon where three locations were
176 used, see Appendix One Table S1.1) DNA was amplified for five mitochondrial genes (12S,
177 overlapping ATPase 8 and 6, ND2, COI) and five nuclear genes (FIB7, PARK7, IRF2,
178 CRYAA, RAPGEF1) (following Kennedy & Spencer, 2014; Kennedy et al., 2019). The
179 phylogenetic dataset's primer details are shown in Table S1 of Kennedy et al. (2019). To
180 investigate within taxon diversity control region (CR) sequences were amplified for multiple
181 individuals per location (except for two taxa where only a single individual was able to be
182 used, see Appendix One Table S1.2) (following Rawlence et al., 2014). Negative controls
183 were included with each PCR reaction. PCR products were purified using the Ultra-Sep Gel
184 extraction kit (Omega) and sequenced on an Applied Biosystems 3730 capillary sequencer.
185 Newly generated sequences for the phylogenetic and CR datasets were added to, and aligned
186 with, those previously published (Kennedy & Spencer, 2014; Rawlence et al., 2014;
187 Rawlence et al., 2017) (see Appendix One Tables S1.1-S1.2).

188   2.2 Phylogenetic and demographic analysis

189 The phylogenetic dataset was divided into nine partitions, five nuclear loci and four
190 mitochondrial loci (the overlapping ATPase 8 and 6 were treated as a single ATPase
191 partition). Models of nucleotide substitution were selected using the Akaike Information
192 Criterion of Modeltest 3.7 (Posada & Crandall, 1998). The models selected for each gene
193 region were: HKY + I for 12S (2st + I), GTR + I for ATPase (6st + I), TIM + G for ND2 (6st
194 + G), TIM + I for COI (6st + I), HKY + I for FIB7 (2st + I), HKY for PARK7 (2st), TrN for
195 IRF2 (6st), HKY for CRYAA (2st), and HKY + I for RAPGEF1 (2st + I). We used
196 StarBEAST2 (v. 0.15.13) implemented in BEAST 2.6.3 (Bouckaert et al., 2019) to jointly
197 infer the *Leucocarbo* species tree along with mitochondrial and individual nuclear gene trees.
198 We implemented an analytical population size integration model (Bouckaert et al., 2019),
199 unlinked substitution models for all partitions, linked trees for mitochondrial genes, and a
200 birth-death tree prior. Strict molecular clocks were used; one linked clock for nuclear genes
201 and unlinked clocks for mitochondrial genes. The clock rates for mitochondrial genes were
202 modelled as normal priors with mean substitution rate estimated from rates for terminal nodes
203 33 to 39 (i.e., the clade *Leucocarbo* belongs to) in Figure S2 of Pacheco et al. (2011)
204 (Appendix One Table S1.3). Mutation rates for individual nuclear genes were modelled with

6

205　1/X priors. We ran three independent MCMC chains, each run for 50 million steps, sampling
206　every 5,000 steps. Additionally, to estimate per species population sizes, analyses were rerun
207　using the linear with constant root populations model with the same parameters, but
208　increasing the MCMC chain to 100 million steps, sampling every 10,000 steps. We checked
209　for convergence and sufficient sampling of parameters in Tracer v1.7.1 (Rambaut et al.,
210　2018) and combined individual runs after discarding the first 10% of steps as burn-in in
211　LogCombiner. Maximum clade credibility consensus trees were generated in TreeAnnotator
212　using the median node age. DensiTree v2.2.7 (Bouckaert, 2010) was used to simultaneously
213　visualise all trees post burn-in and generate consensus trees scaled by estimated effective
214　population size.

215　　　　　2.3 Ancestral range distribution estimation

216　We estimated the ancestral range of internal nodes of the *Leucocarbo* species tree using the R
217　package BioGeoBears (Matzke, 2013). We implemented three methods of ancestral state
218　estimation with and without the jump dispersal parameter (J) (Matzke, 2014), and the
219　dispersal probability as a function of the distance parameter (X) (van Dam & Matzke, 2016):
220　dispersal-extinction-cladogenesis (DEC) (Ree & Smith, 2008), dispersal vicariance analysis
221　(DIVA) (Ronquist, 1997), and Bayesian analysis of biogeography (BAYAREA) (Landi et al.,
222　2013). We compared models using corrected Akaike Information Criterion (AICc) and the
223　weighted AICc values. Due to the criticism of +J models (Ree & Sanmartin, 2018), especially
224　regarding statistical comparison to non-+J models, we did not statistically compare models
225　with and without the +J parameter. We split the samples into seven biogeographic areas: N)
226　North America, S) South America (including the Falkland/Malvinas Islands), O) South
227　Orkney Islands, South Georgia and the South Sandwich Islands, A) Antarctic Peninsula, K)
228　Kerguelen, Heard, Marion and Crozet islands, M) Macquarie Island, and Z) New Zealand and
229　the New Zealand sub-Antarctic islands. For models including the +X parameter, pairwise
230　distances between geographic areas were estimated using Google Earth and normalized
231　against the shortest pairwise distance. All analyses were non-stratified with equal transition
232　between areas.

233　　　　　2.4 Median Joining Network of mitochondrial control region data

234　PopArt (Leigh & Bryant, 2015) was used to construct a median joining network of the
235　mitochondrial control region (CR) data. Sites with >5% unidentified states were masked in
236　the analysis.

237
238　**3.　RESULTS**

239　　　　　3.1 Recent divergence and demographic expansion at high latitudes

240　*Leucocarbo* mitochondrial and nuclear sequences were obtained from across the geographical
241　distribution of blue-eyed shags (and two outgroups, see Appendix One Table S1.1). Of the
242　8200 characters in the partitioned mitochondrial and nuclear dataset, 7727 were constant,
243　while 282 out of 437 variable characters were parsimony informative.

244　*Leucocarbo* shags form a strongly supported monophyletic clade diverging from
245　*Nannopterum* 13.3 Mya (HPD 19.8-8.3 Mya) during the mid-Miocene (Fig. 1). All major
246　clades within the species tree show moderate to strong support (0.85-1.0 PP). The rock shag
247　(*L. magellanicus*) is sister to the remainder of the genus, the split occurring 7.5 Mya (HPD

248   10.9-4.9 Mya) during the late-Miocene, whereas the lineage leading to the Guanay shag (*L.*
249   *bougainvillii*) diverged much more recently 2.6 Mya (HPD 3.9-1.6 Mya) coincident with the
250   onset of the Pleistocene Ice Age 2.58 Mya (Fig. 1). Within the rock shag there is
251   phylogeographic structure dividing populations from the Atlantic (Argentina) and Pacific
252   (Chile) coasts, dating to 1.3 Mya (HPD 2.2-0.01 Mya) (Fig. 1) in agreement with previously
253   reported mitochondrial data (Calderon et al., 2014) and plumage differences (Rasmussen,
254   1987). However, microsatellite data suggests recent secondary contact and geneflow from the
255   Pacific to Atlantic coasts (Calderon et al., 2014).

256   The remaining *Leucocarbo* lineage (leading to all the other extant species) split into two
257   major clades 2.3 Mya (HPD 3.3-1.5 Mya) during the early Pleistocene, shortly after its
258   separation from the Guanay shag lineage (hence the small inter-nodal distance and low
259   posterior probability, PP). The first of these clades contains species from the New Zealand
260   region, while the second comprises taxa from the sub-Antarctic, including South America
261   (and Falkland/Malvinas Islands), Antarctic Peninsula and high latitude sub-Antarctic islands
262   (Fig. 1). Within the sub-Antarctic clade, there are three subclades, the first consisting of
263   species from South America, Falkland/Malvinas Islands, South Georgia and South Orkney
264   Islands; and second (and third) clade comprising taxa from the Antarctica Peninsula, Marion
265   Island, Crozet Island, and Kerguelen, Heard and Macquarie islands, respectively. The Crozet
266   shag (*L. melanogenis*), which inhabits both Crozet and Marion islands, is paraphyletic (Fig.
267   1).

268   DensiTree analysis, which shows congruence or conflict among individual gene-tree
269   topologies, shows broad congruence for the major splits in the species tree (Appendix One
270   Fig. S1.1-1.2). However, there are conflicts within the two major clades within *Leucocarbo*,
271   and the relative placement of some taxa (e.g. Bounty Island shag, *L. ranfurlyi* and New
272   Zealand king shag, *L. carunculatus*).

273   While PP support within the major New Zealand and sub-Antarctic clades is low (*cf.*
274   mitochondrial species tree; Appendix One Fig. S1.1), phylogenetic analyses revealed
275   substantially deeper divergences among temperate *Leucocarbo* lineages relative to those
276   among sub-Antarctic lineages of this genus (Fig. 1). The branch lengths in the New Zealand
277   clade are up to four times longer (up to 2 Mya in the early Pleistocene versus up to 0.5 Mya
278   in the mid-Pleistocene). For instance, while the vast majority of divergence time HPD's
279   among New Zealand taxa substantially predate the LGM, several sub-Antarctic taxa yielded
280   divergence HPDs that are potentially consistent with post-LGM recolonization (Appendix
281   One Table S1.4).

282   Demographic analysis based on the species tree shows stable or increasing population size for
283   blue-eyed shags in South America, compared to founder event induced bottlenecks and
284   subsequent population expansions associated with island endemics (Appendix One Fig.
285   S1.3). The finding of relatively short, potentially post-LGM branch lengths in the sub-
286   Antarctic clade (Fig. 1), is also mirrored to some extent by these demographic reconstructions
287   that reveal recent population expansions in numerous sub-Antarctic lineages following major
288   late-Quaternary bottlenecks (Appendix One Fig. S1.3).

289   In the mitochondrial CR dataset, there were 1026 characters, of which 925 were constant,
290   while 83 out of 101 variable characters were parsimony informative. The median joining
291   network of fast-evolving mitochondrial CR sequences from multiple individuals for the

292 majority of each *Leucocarbo* species (Appendix One Fig. S1.4) shows deep, clear separation
293 of rock and Guanay shags and those from the New Zealand region in contrast to the blue-
294 eyed shags from the sub-Antarctic clade. All species of blue-eyed shags form their own
295 genetic clusters for the CR data, with the exception of the Crozet shag (*L. melanogenis*).
296 There are shallow to deep (e.g. rock shag) levels of genetic variation within blue-eyed shags,
297 with the exception of the Campbell (*L. campbelli*), Auckland (*L. colensoi*), Bounty (*L.*
298 *ranfurlyi*), and Macquarie (*L. purpurascens*) Island shags, where single haplotypes are
299 present. The blue-eyed shag CR substitution rate of 3.2 s/s/Ma (95% HPD 0.70-6.57;
300 Rawlence et al., 2015) suggests divergence dates broadly consistent with those determined in
301 our phylogenetic analysis of nuclear and mitochondrial DNA markers.

302   3.2 Founder event speciation

303 The best-supported BioGeoBears evolutionary scenario for blue-eyed shags, based on our
304 phylogenetic analysis, was a jump dispersal (founder-event speciation) – extinction –
305 cladogenesis (DEC+J) model (Fig. 1, Appendix One Table S1.5). This founder-speciation
306 model reconstructed an ancestral geographical area for *Leucocarbo* of South America, and
307 for all major nodes in the phylogeny. The inferred most-recent common ancestor of the two
308 major clades within *Leucocarbo* is from South America, with subsequent circumpolar
309 expansion supported by the Antarctic Circumpolar Current (ACC). The best-supported
310 scenario without a jump parameter was DEC (expansion and speciation) (Appendix One Fig.
311 S1.5, Table S1.5). In contrast to DEC+J, ancestors at deeper nodes in the phylogeny are
312 inferred to have been geographically widespread, with temporally offset *in situ* speciation on
313 different islands.

314

315 **4. DISCUSSION**

316 Genetic analysis of *Leucocarbo* shags reveals a remarkably shallow evolutionary history
317 among endemic lineages breeding at island groups scattered across the vast Southern Ocean,
318 consistent with a recent high-latitude circumpolar radiation. This rapid sub-Antarctic
319 archipelagic expansion contrasts with significantly deeper lineages detected at temperate
320 latitudes in South America and New Zealand that may have acted as glacial refugia. Recent
321 high-latitude expansions are further supported by ancestral demographic and biogeographic
322 reconstructions.

323   4.1 Postglacial circumpolar expansion

324 The shallow phylogenetic history of sub-Antarctic *Leucocarbo* (Fig. 1) relative to mid-
325 latitude lineages in the New Zealand region (up to 2 Mya) and South America (up to 7.5
326 Mya) almost certainly reflects the impact of repeated glacial-interglacial cycles during the
327 Pleistocene (2.58 – 0.01 Mya) in underpinning Southern Ocean extinction-recolonization
328 events (Fraser et al., 2009; Nikula et al., 2010; Fraser et al., 2012). Specifically, our analysis
329 detected a four-fold difference in branch lengths between the two major clades of *Leucocarbo*
330 (Fig. 1), with deep phylogenetic histories detected among temperate lineages in putative
331 glacial refugia (e.g., New Zealand islands). This recent expansion history of sub-Antarctic
332 taxa to previously ice-bound, potentially glaciated islands is further highlighted by latitudinal
333 contrasts in demographic reconstructions (Appendix One Fig. S1.3) and echoes recent

334 demographic comparisons of other iconic Southern Ocean seabirds with circumpolar
335 distributions (Trucchi et al., 2014; Cole et al., 2019).

336 Circumpolar dispersal events (Fig. 1) were likely facilitated by the ACC and westerly winds
337 encircling Antarctica (Fraser et al., 2012). While dating of the shallowest phylogenetic nodes
338 is likely confounded by population-level time-dependant processes (Burridge et al., 2009)
339 (making disentangling the effects of repeated Pleistocene glacial-interglacial cycles difficult),
340 the short internodal distances between far-flung lineages of the Southern Ocean (e.g.
341 Macquarie versus Kerguelen; Antarctic Peninsula versus Marion Island), separated in some
342 instances by ~10,000 km, could correspond to colonization events in several of the recent
343 post-glacial periods. The shortest internodal distances likely reflect post-LGM dispersal (Fig.
344 1). Indeed, as a proxy for earlier glacial periods, these southern coasts are hypothesized to
345 have been heavily affected by LGM winter sea ice (Ehlers et al., 2011), and in some cases ice
346 and snow cover (Hodgson et al., 2014), which extended north of the current route of the
347 Antarctic Polar Front (Fig. 1; Fraser et al., 2009). In addition to its impact on coastal benthic
348 and intertidal species (Fraser et al., 2009; Nikula et al., 2010; Gonzalez-Wevar et al., 2018),
349 extensive sea ice during glacial maxima is thought to have extirpated Southern Ocean avian
350 lineages that depend on coastal ecosystems (Trucchi et al., 2014; Cole et al., 2019).
351 *Leucocarbo* shags are inshore foragers largely dependent on benthic species which they hunt
352 through pursuit-diving (Cook et al., 2013). Limited by dive depth and foraging range, blue-
353 eyed shags are particularly prone to ecosystem disturbance (Cook et al., 2013; Rawlence et
354 al., 2016), though less so than intertidal species in this context (de Bruyn et al., 2009; Fraser
355 et al., 2009; Gonzalez-Wevar et al., 2018) (as their presence on the seasonally ice-impacted
356 Antarctic Peninsula indicates). Our phylogeographic analyses (Fig. 1) strongly suggest that
357 the New Zealand region and unglaciated South America (including the Falkland/Malvinas
358 Islands) both acted as key glacial refugia, consistent with previous analyses (Austin et al.,
359 2013; Cole et al., 2019; Rexer-Huber et al., 2019).

360 The inferred postglacial expansion out of South America involved two large-scale, rapid
361 dispersal events: the first from the South American mainland (including Falkland/Malvinas
362 Islands) to the archipelagos of South Georgia and South Orkney Islands (resolving any
363 ambiguity about the origin of the South Orkney Islands shags; Schrimpf et al., 2018); and the
364 other from the mainland to the Antarctic Peninsula and into the high-latitude sub-Antarctic
365 islands (Fig. 1). Founder-takes-all (or density-dependent) processes (Waters et al., 2013) may
366 help to explain some of these idiosyncratic expansion patterns, notably the failure of the
367 South Georgia shag (*L. georgianus*) to colonize the Antarctic Peninsula (where the Antarctic
368 shag *L. bransfieldensis* breeds), and the absence of close relatives of the Macquarie Island
369 shag (*L. purpurascens*) in the New Zealand region, a mere 500km downwind. However, more
370 complicated dispersal scenarios cannot be discounted given the conflict among gene trees
371 (due to incomplete lineage sorting and/or gene-flow), and between the species tree (Fig. 1)
372 and the mitochondrial CR data (Appendix One Fig. S1.4). Indeed, the South American and
373 Falkland/Malvinas Island forms of the imperial shag (*L. atriceps*, sometimes treated as
374 subspecies *atriceps* and *albiventer*, respectively, e.g. Nelson, 2005) are paraphyletic (in
375 comparison to the monophyly exhibited by the other *Leucocarbo* spp., see Appendix One Fig.
376 S1.4), and no doubt represent the same taxon (see also Calderon et al., 2014). This situation
377 makes it difficult to infer whether blue-eyed shags that dispersed to other islands in the
378 Southern Ocean and the Antarctic continent came from the South American mainland or the

379   nearby Falkland/Malvinas Islands. Regardless, like *Leucocarbo* species in the New Zealand
380   clade, this postglacial dispersal is characterized by the genetic signatures of founder-events
381   and associated population bottlenecks followed by subsequent population expansions.

382

383   4.2 Rapid founder speciation

384   Evolutionary biogeographic reconstructions strongly support a founder-speciation model
385   (jump dispersal) for all major nodes of the *Leucocarbo* phylogeny. Indeed, the 'jump'
386   parameter is important in modelling founder-event speciation events that often characterize
387   remote archipelagic species (Matzke, 2014; see also Ree & Sanmartin, 2018). By contrast,
388   the best-supported alternative evolutionary scenario lacking such a jump parameter requires
389   widespread ancestors at deeper nodes, which seems biogeographically implausible in this
390   region (Appendix One Figure S1.5, Table S1.4).

391   Founder speciation represents a fascinating feature of archipelagic biogeography globally
392   (Mendelson & Shaw, 2005; Shaw & Gillespie, 2016), and such phenomena may be heavily
393   influenced by density-dependent processes (Waters et al., 2013; Shaw & Gillespie, 2016).
394   While many of the best-known archipelagic radiations have been detected in tropical systems
395   that have been relatively sheltered from global climatic shifts, our study suggests that such
396   founder-speciation processes may be important even in the vast Southern Ocean (Trucchi et
397   al., 2014; Cole et al., 2019; Baird et al., 2021), a system heavily impacted by geologically
398   recent glacial cycles. Indeed, the apparent pace of colonization and speciation, including
399   previously unrecognized founder events, in Southern Ocean *Leucocarbo* may approach that
400   of the most rapid radiations elsewhere in the globe (Kornfield, 1978; Mendelson & Shaw,
401   2005; Momigliano et al., 2017; Puntambekar et al., 2020; Turbek et al., 2021). We note that a
402   recent field guide to seabirds (Harrison et al., 2021) depicts significant differences in adult
403   breeding plumage and skin colouration (e.g. extent of white feathering on the cheek, gular
404   colour, size and colour of the carunculation above the bill) among the various species. These
405   differences, composites of details observable in recent detailed digital photographs (Peter
406   Harrison pers. comm.), are likely to be critical in specific-mate recognition.

407   The Crozet Island shag (*L. melanogenis*), originally described from Crozet Island, but also
408   seemingly present on Marion Island (Blyth, 1860; Moseley, 1879; Alexander, 1928;
409   Holgersen, 1945; Crawford, 1952; Rand, 1954; Rand, 1956; Crawford et al., 2003), is
410   paraphyletic in our analyses (Fig. 1, Appendix One Fig. S1.4), and is possibly the
411   consequence of an unrecognized founder event on Marion Island. Considering the observed
412   plumage differences between blue-eyed shags from Marion and Crozet Islands (Rand, 1954),
413   and phylogeographic structure within *Leucocarbo*, we suggest that the Marion Island
414   population may represent a new undescribed taxon.

415   It is not clear, however, how *Leucocarbo* shags managed to colonize remote island groups,
416   separated by thousands of kilometres, across an expanse of empty ocean. Shag biology
417   suggests a relatively low dispersal capacity. Like other species in Phalacrocoracidae,
418   *Leucocarbo* shags have a partially wettable plumage that decreases the layer of insulating air
419   and reduces the energetic costs of diving (Gremillet et al., 2005; Cook & Leblanc, 2007).
420   Blue-eyed shags would not be expected to withstand days or weeks at sea in cold Southern
421   Ocean waters, although facultative hypothermia observed in these shags might enable some

422 tolerance to near-freezing sea-water temperatures (Bevan et al., 1997). Flight performance in
423 this group is also rather limited compared to other avian lineages (Pennycuick, 1989), in part
424 due to their dense bones, which aid in diving. A several thousand-kilometre non-stop flight
425 across the Southern Ocean would therefore seem unlikely, unless driven by some particularly
426 strong and sustained westerly wind and current system. Furthermore, due to the depth of the
427 Southern Ocean, access to benthic prey would be impossible during stopovers on the water
428 surface, although *Leucocarbo* shags are flexible enough to occasionally forage on pelagic fish
429 species (Cook et al., 2013).

430 It is possible that blue-eyed shags dispersed eastwards from South America following the
431 frontline of the receding sea-ice after glacial maxima and were thus able to approach recently
432 ice-freed remote sub-Antarctic islands more easily. Regardless of the colonization or re-
433 colonization pathway, it is a distinct possibility that the sub-Antarctic islands were colonized
434 by small groups of shags (10-20 birds), rather than by lone individuals, as blue-eyed shags
435 will readily forage or travel in groups (Cook et al., 2013).

436   4.3 Sentinels of change

437 Intriguingly, *Leucocarbo* shags exhibit a mixture of biological characteristics seen in both
438 poorly and highly dispersive taxa. The phylogeographic pattern of multiple deep lineages in
439 the New Zealand region and South America, versus shallow lineages in Antarctica and high-
440 latitude sub-Antarctic islands, provides a clear signature of rapid expansions from ice-free
441 refugia into previously glaciated and/or ice-bound areas (Fraser et al., 2012), and strongly
442 indicates a sensitivity to climate change. The strong philopatric behaviour of *Leucocarbo*
443 shags has resulted in high levels of endemism, a pattern that might be expected for less
444 dispersive taxa (Gonzalez-Wevar et al., 2017; Gonzalez-Wevar et al., 2019; Rexer-Huber et
445 al., 2019; Baird et al., 2021). The circumpolar distribution of blue-eyed shags, and their
446 highly dynamic evolutionary history in relation to climate change (Calderon et al., 2014; this
447 study) and anthropogenic impacts (Rawlence et al., 2014; Rawlence et al., 2015; Rawlence et
448 al., 2017), potentially make *Leucocarbo* a strong sentinel of past and ongoing Southern
449 Ocean ecosystem change.
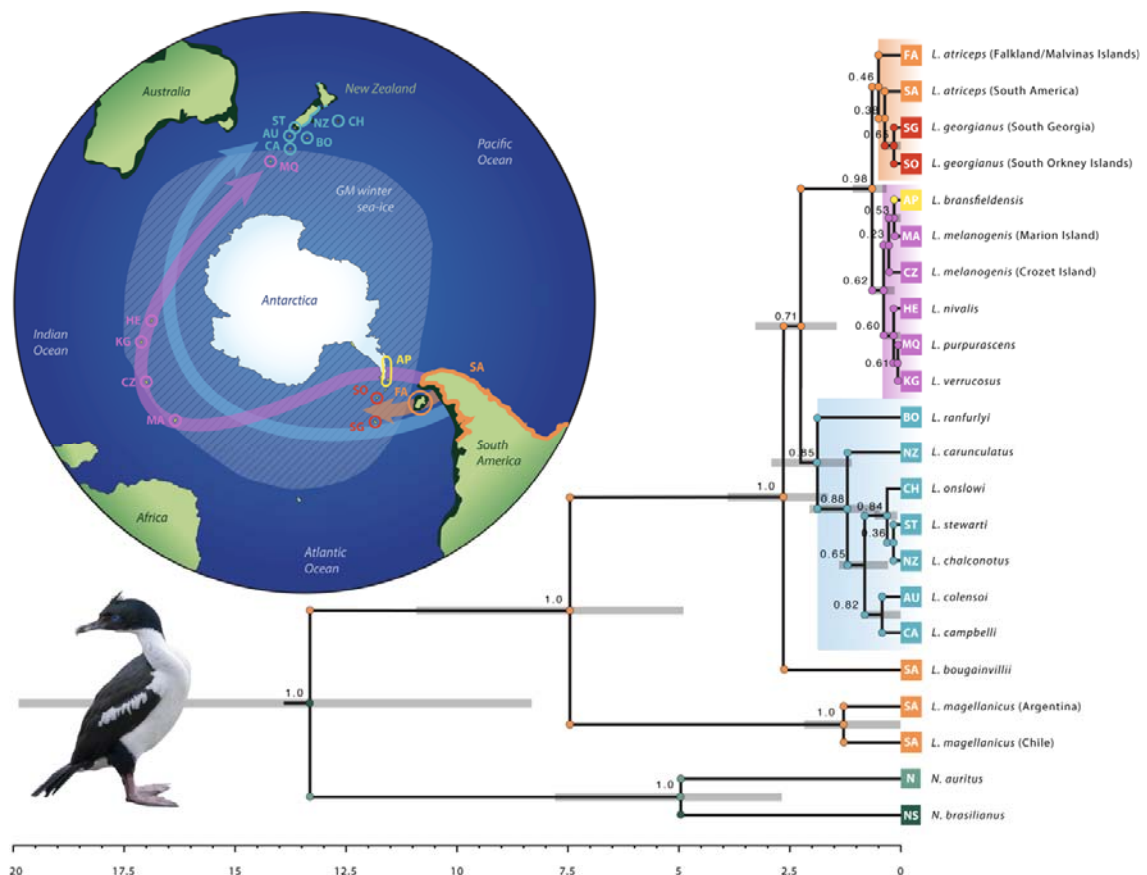
Figure 1 Evolutionary history of blue-eyed shags (*Leucocarbo* spp.) in the Southern Ocean. The map depicts inferred postglacial colonization routes (arrows) supported by the dominant westerly winds and eastward flow of the Antarctic Circumpolar Current. The extent of winter sea ice (cross-hatched pattern) and land area (dark green) during the Pleistocene Last Glacial Maximum 29-19 Kya is indicated. Rapid circumpolar expansion and founder speciation hypotheses are supported by temporal phylogenetic and ancestral biogeographic reconstructions. The time-calibrated species tree is derived from 8.2 kilobases of DNA sequence data (five mitochondrial and five nuclear genes) with *Nannopterum* as the outgroup. Node bars on the phylogeny are 95% HPD of divergence times as indicated on the scale bar (millions of years before present). Node values are Bayesian posterior probability support. Node circles are the ancestral state reconstruction of the geographic distribution based on the DEC+J model. Colours and abbreviations are as follows: orange: South America; purple: high-latitude sub-Antarctic islands; yellow: Antarctic Peninsula; blue: New Zealand region; olive: North America; dark green: South America; FA: Falkland/Malvinas Islands; SA: South America; SG: South Georgia; SO: South Orkney Islands: AP: Antarctic Peninsula; MA: Marion Island; CZ: Crozet Island; HE: Heard Island; MQ: Macquarie Island; KG: Kerguelen Island; CA: Campbell Island; AU: Auckland Island; NZ: mainland New Zealand; ST: Stewart Island; CH: Chatham Islands; BO: Bounty Islands; N: North America; NS: North and South America. Clade and arrow colours: orange: South America, South Georgia, South Orkney Islands; purple: Antarctic Peninsula, high-latitude sub-Antarctic islands; blue: New Zealand region.

REFERENCES

Alexander, W. B. (1928). Birds of the ocean: A handbook for voyagers, containing descriptions of all the sea-birds of the world, with notes on their habits and guides to their identification. New York: Putnam.

Austin, J. J., Soubrier, J., Prevosti, F. J., Prates, L., Trejo, V., Mena, F., & Cooper, A. (2013). The origins of the enigmatic Falklands Islands wolf. *Nature Communications*, 4, 1552.

Baird, H. P., Shin, S., Oberprieler, R. G., Hulle, M., Vernon, P., Moon, K. L., Adams, R. H., McKenna, D. D., & Chown, S. L. (2021). Fifty million years of beetle evolution along the Antarctic Polar Front. *PNAS*, 118, e2017384118.

Bevan, R. M., Boyd, I. L., Butler, P. J., Reid, K., Woakes, A. J., & Croxall, J. (1997). Heart rates and abdominal temperatures of free-ranging South Georgian shags, *Phalacrocorax georgianus*. *Journal of Experimental Biology*, 200, 661–675.

Blyth, E. (1860). Report of the curator, Zoological Department. *Journal of the Asiatic Society of Bengal*, 29, 87-115.

Bouckaert, R. R. (2010). DensiTree: Making sense of sets of phylogenetic trees. *Bioinformatics*, 26, 1372-1373.

Bouckaert, R., Vaughan, T. G., Barido-Sottani, J., Duchene, S., Fourment, M., Gavryushkina, A., Heled, J., Jones, G., Kuhnert, D., de Maio, N., Matschiner, M., Mendes, F. K., Muller, N. F., Ogilvie, H. A., du Plessis, L., Popinga, A., Rambaut, A., Rasmussen, D., Siveroni, I., Suchard, M. A., Wu, C. H., Xie, D., Zhang, C., Stadler, T., & Drummond, A. J. (2019). BEAST 2.5: An advanced software platform for Bayesian evolutionary analysis. *PLoS Computational Biology*, 15, e1006650.

de Bruyn, M., Hall, B. L., Chauke, L. F., Baroni, C., Koch, P. L., & Hoelzel, A. R. (2009). Rapid response of a marine mammal species to Holocene climate and habitat change. *PLoS Genetics*, 5, e1000554.

Burridge, C. P., Craw, D., Fletcher, D., & Waters, J. M. (2009). Geological dates and molecular rates: fish DNA sheds light on time dependency. *Molecular Biology and Evolution*, 25, 624-633.

Calderón, L., Quintana, F., Cabanne, G. S., Lougheed, S. C., & Tubaro, P. L. (2014). Phylogeography and genetic structure of two Patagonian shag species (Aves: Phalacrocoracidae). *Molecular Phylogenetics and Evolution*, 72, 42–53.

Carrea, C., Burridge, C. P., Wienecke, B., Emmerson, L. M., White, D., & Miller, K. J. (2019). High vagility facilitates population persistence and expansion prior to the Last Glacial Maximum in an Antarctic top predator: the snow petrel (*Pagodroma nivea*). *Journal of Biogeography*, 46, 442-453.

Chen, I. C., Hill, J. K., Ohlemuller, R., Roy, D. B., & Thomas, C. D. (2011). Rapid range shifts of species associated with high levels of climate warming. *Science*, 333, 1024-1026.

Cole, T. L., Dutoit, L., Dussex, N., Hart, T., Alexander, A., Yonger J. L., Clucas, G. V., Frugone, M. J., Cherel, Y., Cuthbert, R., Ellenberg, U., Fiddaman, S. R., Hiscock, J., Houston, D., Jouventin, P., Mattern, T., Miller, G., Miskelly, C., Nolan, P., Polito, M. J., Quillfeldt, P., Ryan, P. G., Smith, A., Tennyson, A. J. D., Thompson, D., Wienecke, B.,

514 Vianna, J. A., & Waters, J. M. (2019). Receding ice drove parallel expansions in Southern
515 Ocean penguins. *PNAS*, 116, 26690-26696.

516 Cook, T. R., & Leblanc, G. (2007). Why is wing-spreading behaviour absent in blue-eyed
517 shags? *Animal Behaviour*, 74, 649-652.

518 Cook, T. R., Lescroël, A., Cherel, Y., Kato, A., & Bost, C-A. (2013). Can foraging ecology
519 drive the evolution of body size in a diving endotherm? *PLoS ONE*, 8, e56297.

520 Crawford, A. B. (1952). The birds of Marion Island, South Indian Ocean. *Emu*, 52, 73-85.

521 Crawford, R. J. M., Cooper, J., Dyer, B. M., Wolfaardt, A. C., Tshingana, D., Spencer, K.,
522 Petersen, S. L., Nel, J. L., Keith, D. G., Holness, C. L., Hanise, B., Greyling, M. D., & Du
523 Toit, M. (2003). Population, breeding, diet and conservation of the Crozet Shag
524 *Phalacrocorax [atriceps] melanogenis* at Marion Island, 1994/95–2002/03. *African Journal*
525 *of Marine Science*, 25, 537-547.

526 van Dam, M. H., & Matzke, N. J. (2016). Evaluating the influence of connectivity and
527 distance on biogeographical patterns in south-western deserts of North America. *Journal of*
528 *Biogeography*, 43, 1514-1532.

529 Davis, M. B., & Shaw, R. G. (2001). Range shifts and adaptive responses to Quaternary
530 climate change. *Science*, 292, 673-679.

531 Ehlers, J., Gibbard, P. L., & Hughes, P. D. (2011). Quaternary glaciations – extent and
532 chronology. *Developments in Quaternary Science* 15. Elsevier.

533 Fraser, C. I., Morrison, A. K., Hogg, A. M., Macaya, E. C., van Sebille, E., Ryan, P. G.,
534 Padovan, A., Jack, C., Valdivia, N., & Waters, J. M. (2018). Antarctica's ecological isolation
535 will be broken by storm-driven dispersal and warming. *Nature Climate Change*, 8, 604-708.

536 Fraser, C. I., Nikula, R., Ruzzante, D. E., & Waters, J. M. (2012). Poleward bound: biological
537 impacts of Southern Hemisphere glaciation. *Trends in Ecology and Evolution*, 27, 462-471.

538 Fraser, C. I., Nikula, R., Spencer, H. G., & Waters, J. M. (2009). Kelp genes reveal effects of
539 subantarctic sea ice during the Last Glacial Maximum. *PNAS*, 106, 3249-3253.

540 Fraser, C. I., Nikula, R., & Waters, J. M. (2011). Oceanic rafting by a coastal community.
541 *Proceedings B*, 278, 649-655.

542 Fraser, C. I., Thiel, M., Spencer, H. G., & Waters, J. M. (2010). Contemporary habitat
543 discontinuity and historic glacial ice drive genetic divergence in Chilean kelp. *BMC*
544 *Evolutionary Biology*, 10, 203.

545 Gersonde, R., Crosta, X., Abelmann, A., & Armand, L. (2005). Sea-surface temperature and
546 sea ice distribution of the Southern Ocean at the Last Glacial Maximum – a circum-Antarctic
547 view based on siliceous microfossil records. *Quaternary Science Reviews*, 24, 869-896.

548 González-Wevar, C. A., Hüne, M., Rosenfeld, S., Nakano, T., Saucède, T., Spencer, H. G., &
549 Poulin, E. (2019) Systematic revision of *Nacella* (Patellogastropoda: Nacellidae) based on a
550 complete phylogeny of the genus, with the description of a new species from the southern tip
551 of South America. *Zoological Journal of the Linnean Society*, 186, 303-336.

552 González-Wevar, C. A., Hüne, M., Segovia, N. I., Nakano, T., Spencer, H. G., Chown, S. L.,
553 Saucede, T., Johnstone, G., Mansilla, A., & Poulin, E. (2017). Following the Antarctic
554 Circumpolar Current: patterns and processes in the biogeography of the limpet *Nacella*
555 (Mollusca: Patellogastropoda) across the Southern Ocean. *Journal of Biogeography*, 44, 861-
556 874.

557 González-Wevar, C. A., Segovia, N. I., Rosenfeld, S., Ojeda, J., Hüne, M., Naretto, J.,
558 Saucede, T., Brickle, P., Morley, S., Feral, J. P., Spencer, H. G., & Poulin, E. (2018).
559 Unexpected absence of island endemics: long-distance dispersal in higher latitude sub-
560 Antarctic *Siphonaria* (Gastropoda: *Euthyneura*) species. *Journal of Biogeography*, 45, 874-
561 884.

562 Grémillet, D., Chauvin, C., Wilson, R. P., Le Maho, Y., & Wanless, S. (2005). Unusual
563 feather structure allows partial plumage wettability in diving great cormorants *Phalacrocorax*
564 *carbo*. *Journal of Avian Biology*, 36, 57-63.

565 Harrison, P., Perrow, M. R., & Larsson, H. (2021). Seabirds: The new identification guide.
566 Barcelona: Lynx Edicions.

567 Hewitt, G. (2000). The genetic legacy of the Quaternary ice ages. *Nature*, 405, 907-913.

568 Hodgson, D. A., Graham, A. G. C., Roberts, S. J., Bentley, M. J., Cofaigh, C. O., Verleyen,
569 E., Vyverman, W., Jomelli, V., Favier, V., Brunstein, D., Verfaillie, D., Colhoun, E. A.,
570 Saunders, K. M., Selkirk, P. M., Mackintosh, A., Hedding, D. W., Nel, W., Hall, K.,
571 McGlone, M. S., van der Putten, S., Dickens, W. A., & Smith, J. A. (2014). Terrestrial and
572 submarine evidence for the extent and timing of the Last Glacial Maximum and the onset of
573 deglaciation on the maritime-Antarctic and sub-Antarctic islands. *Quaternary Science*
574 *Reviews*, 100, 137-158.

575 Holgersen, H. (1945). Antarctic and sub-antarctic birds. Scientific results of the Norwegian
576 Antarctic expeditions 1927-1928. Oslo.

577 Kennedy, M., Seneviratne, S. S., Mendis, U. K., & Spencer, H. G. (2019). Sorting out the
578 Snakebirds: The species status, phylogeny and biogeography of the Darters (Aves:
579 Anhingidae). *Journal of Zoological Systematic and Evolutionary Research*, 57, 892–899.

580 Kennedy, M., & Spencer, H. G. (2014). Classification of the cormorants of the world.
581 *Molecular Phylogenetics and Evolution*, 79, 249-257.

582 Kornfield, I. L. (1978). Evidence for rapid speciation in African cichlid fishes. *Experientia*,
583 34, 335-336.

584 Landi, M. J., Matzke, N. J., Moore, B. R., & Huelsenbeck, J. P. (2013). Bayesian analysis of
585 biogeography when the number of areas is large. *Systematic Biology*, 62, 789-804.

586 Leigh, J. W., & Bryant, D. (2015). PopART: full-feature software for haplotype network
587 construction. *Methods in Ecology and Evolution*, 6, 1110-1116.

588 Maggs, C. A., Castilho, R., Foltz, D., Henzler, C., Jolly, M. T., Kelly, J., Olsen, J., Perez, K.
589 E., Stam, W., Vainola, R., Vaird, F., & Wares, J. (2008). Evaluating signatures of glacial
590 refugia for North Atlantic benthic marine taxa. *Ecology*, 89, S108-S122.

591 Matzke, N. (2013). Probabilistic historical biogeography: new models for founder-event
592 speciation, imperfect detection, and fossils allow improved accuracy and model-testing.
593 *Frontiers in Biogeography*, 5, 242-248.

594 Matzke, N. J. (2014). Model selection in historical biogeography reveals that founder-event
595 speciation is a crucial process in island clades. *Systematic Biology*, 63, 951-970.

596 Mendelson, T. C., & Shaw, K. L. (2005). Sexual behaviour: rapid speciation in an arthropod.
597 *Nature*, 433, 375-376.

598 Momigliano, P., Jokinen, H., Fraimout, A., Florin, A. B., Norkko, A., & Merila, J. (2017).
599 Extraordinarily rapid speciation in a marine fish. *PNAS*, 114, 6074-6079.

600 Moseley, H. N. (1879). Notes by a naturalist on the "Challenger," being an account of various
601 observations made during the voyage of H.M.S. "Challenger" round the world, in the years
602 1872-1876. London: Macmillan.

603 Nelson, J. B. (2005). Pelicans, cormorants and their relatives (Pelecanidae, Sulidae,
604 Phalacrocoracidae, Anhingidae, Fregatidae, Phaethontidae). Oxford: Oxford University Press.

605 Nikula, R., Fraser, C. I., Spencer, H. G., & Waters, J. M. (2010). Circumpolar dispersal by
606 rafting in two subantarctic kelp-dwelling crustaceans. *Marine Ecology Progress Series*, 405,
607 221-230.

608 Pacheco, M. A., Battistuzzi, F. U., Lentino, M., Aguilar, R. F., Kumar, S., & Escalante, A. A.
609 (2011). Evolution of modern birds revealed by mitogenomics: Timing the radiation and
610 origin of major orders. *Molecular Biology and Evolution*, 28, 1927-1942.

611 Parmesan, C., & Yohe, G. A. (2003). Globally coherent fingerprint of climate change impacts
612 across natural systems. *Nature*, 421, 37-42.

613 Pennycuick, C. J. (1989). Bird flight performance: A practical calculation manual. Oxford:
614 Oxford University Press.

615 Posada, D., & Crandall, K. A. (1998). MODELTEST: testing the model of DNA substitution.
616 *Bioinformatics*, 14, 817-818.

617 Puntambekar, S., Newhouse, R., Navas, J. S. M., Chauhan, R., Vernaz, G., Willis, T.,
618 Wayland, M. T., Umrania, Y., Miska, E. A., & Prabakaran, S. (2020). Evolutionary
619 divergence of novel open reading frames in cichlids speciation. *Scientific Reports*, 10, 1-18.

620 Rambaut, A., Drummond, A. J., Xie, D., Baele, G., & Suchard, M. A. (2018). Posterior
621 summarization in Bayesian phylogenetics using Tracer 1.7. *Systematic Biology*, 67, 901-904.

622 Rand, R. W. (1954). Notes on the birds of Marion Island. *Ibis*, 96, 173–200.

623 Rand, R. W. (1956). Cormorants on Marion Island. *Ostrich*, 27, 127–133.

624 Rasmussen, P. C. (1987). Molts of the rock shag and new interpretations of the plumage
625 sequence. *The Condor*, 89, 760-766.

626 Rawlence, N. J., Kennedy, M., Anderson, C. N. K., Prost, S., Till, C. E., Smith, I. W. G.,
627 Scofield, R. P., Tennyson, A. J. D., Hamel, J., Lalas, C., Matisoo-Smith, E. A., & Waters, J.

628   M. (2015). Geographically contrasting biodiversity reductions in a widespread New Zealand
629   seabird. *Molecular Ecology*, 24, 4605-4616.

630   Rawlence, N. J., Scofield, R. P., Spencer, H. G., Lalas, C., Easton, L. J., Tennyson, A. J. D.,
631   Adams, M., Pasquet, E., Fraser, C., Waters, J. M., & Kennedy, M. (2016). Genetic and
632   morphological evidence for two species of *Leucocarbo* shag (Aves, Pelecaniformes,
633   Phalacrocoracidae) from southern South Island of New Zealand. *Zoological Journal of the
634   Linnean Society*, 177, 676-694.

635   Rawlence, N. J., Till, C. E., Easton, L. J., Spencer, H. G., Schuckard, R., Melville, D. S.,
636   Scofield, R. P., Tennyson, A. J. D., Rayner, M. J., Waters, J. M., & Kennedy, M. (2017).
637   Speciation, range contraction and extinction in the endemic New Zealand king shag complex.
638   *Molecular Phylogenetics and Evolution*, 115, 197-209.

639   Rawlence, N. J., Till, C. E., Scofield, R. P., Tennyson, A. J. D., Collins, C. J., Lalas, C., Loh,
640   G., Matisoo-Smith, E. A., Waters, J. M., Spencer, H. G., & Kennedy, M. (2014). Strong
641   phylogeographic structure in a sedentary seabird, the Stewart Island shag (*Leucocarbo
642   chalconotus*). *PLoS One*, 9, e90769.

643   Ree, R. H., & Sanmartin, I. (2018). Conceptual and statistical problems with the DEC+J
644   model of founder-event speciation and its comparison with DEC via model selection. *Journal
645   of Biogeography*, 45, 741-749.

646   Ree, R. H., & Smith, S. A. (2008). Maximum likelihood inference of geographic range
647   evolution by dispersal, local extinction, and cladogenesis. *Systematic Biology*, 57, 4-14.

648   Rexer-Huber, K., Veale, A. J., Catry, P., Cherel, Y., Dutoit, L., Foster, Y., McEwan, J. C.,
649   Parker, G. C., Phillips, R. A., Ryan, P. G., Stanworth, A. J., van Stijn, T., Thompson, D. A.,
650   Waters, J., & Robertson, B. C. (2019). Genomics detects population structure within and
651   between ocean basins in a circumpolar seabird: the white-chinned petrel. *Molecular Ecology*,
652   28, 4552-4572.

653   Ronquist, F. (1997). Dispersal-vicariance analysis: A new approach to the quantification of
654   historical biogeography. *Systematic Biology*, 46, 195-203.

655   Schrimpf, M., Naveen, R., & Lynch, H. J. (2018). Population status of the Antarctic shag
656   *Phalacrocorax (atriceps) bransfieldensis*. *Antarctic Science*, 30, 151-159.

657   Shaw, L. K., & Gillespie, R. G. (2016). Comparative phylogeography of oceanic
658   archipelagos: Hotspots for inferences of evolutionary processes. *PNAS*, 113, 7986-7993.

659   Trucchi, E., Gratton, P., Whittington, J. D., Cristofari, R., Maho, Y. L., Stenseth, N. C., &
660   Bohec, C. E. (2014). King penguin demography since the last glaciation inferred from
661   genome-wide data. *Proceedings B*, 281, 20140528.

662   Turbek, S. P., Browne, M., Giacomo, A. S. D., Kopuchian, C., Hochachka, W. M., Estalles,
663   C., Lijtmaer, D. A., Tubaro, P. L., Silveira, L. F., Lovette, I. J., Safran, R. J., Taylor, S. A., &
664   Campagna, L. (2021). Rapid speciation via the evolution of pre-mating isolation in the Ibera
665   seedeater. *Science*, 371, eabc0256.

666   Walsh, P. S., Metzger, D. A., & Higuchi, R. (2013). Chelex 100 as a medium for simple
667   extraction of DNA for PCR-based typing from forensic material. *Biotechniques*, 54, 134–139.

668 Waters, J. M., Fraser, C. I., & Hewitt, G. M. (2013). Founder takes all: density-dependent
669 processes structure biodiversity. *Trends in Ecology and Evolution*, 28, 78-85

670

DATA ACCESSIBILITY

672 Data and scripts to reproduce the results of this study are available on Data Dryad: XXXXX.
673 Sequences have been uploaded to GenBank (see Appendix One Tables S1.1-S1.2).

674

BIOSKETCH

676 **Nic Rawlence** is a biologist who uses genetic tools to study evolutionary processes. His work
677 is primarily focused on reconstructing the impacts of climate change and humans on
678 ecosystems through time.

679 **Author Contributions:** NJR, JMW, HGS, CET and MK developed the study concept. NJR,
680 ATS, JMW, HGS and MK designed the project and wrote the initial manuscript. TRC, C-AB,
681 LJN, PGR, LC, PQ, JFM, NR and RAP collected and/or provided samples. CET, TMK and
682 MK generated the sequence data. ATS, LS, NJR, LD and MK generated results. TRC, LJN,
683 PGR, LC and RAP helped design sampling and project directions. All authors contributed to
684 the final manuscript.